The thesis committee for Dmitry Meyerson

certifies that this is the approved version of the following thesis:

Experimental Measurements of Energy Transport in Tokamak Plasmas

APPROVED BY

SUPERVISING COMMITTEE:

Ken Gentle, Supervisor

Wendell Horton

Experimental Measurements of Energy Transport in Tokamak Plasmas

by

Dmitry Meyerson, A.B.

THESIS

Presented to the Faculty of the Graduate School of

The University of Texas at Austin

in Partial Fulfillment

of the Requirements

for the Degree of

Master of Arts

THE UNIVERSITY OF TEXAS AT AUSTIN

December 2010

Experimental Measurements of Energy Transport in Tokamak Plasmas

Dmitry Meyerson, M.A.
The University of Texas at Austin, 2010

Supervisor: Ken Gentle

A tokamak plasma near equilibrium can be perturbed with modulated power sources, such as modulated electron cyclotron heating, or repeated cold pulse application. Temperature response to cyclical changes in profiles parameters that are induced by modulated power deposition can be used to test theoretical transport models as well as improve experimental phenomenology used to optimize tokamak performance. The goal of this document to discuss some methods of analyzing electron temperature data in the context of energy transport. Specific experiments are considered in order to demonstrate the methods discussed, as well as to examine the electron energy transport properties of these shots.

Electron cyclotron emission provides a convenient way to probe electron temperature for plasmas in thermal equilibrium. We can show that in tokamak devices,barring harmonic overlap, we can associate a particular

frequency with a particular location in a tokamak, by carefully selecting the detection frequency and line of sight of the responsible antenna. ECE radiometers typically measure temperature at tens of locations at a time with a spatial resolution on the order of a few centimeters. Tracking the evolution of electron energy flux depends on careful analysis of the resulting data.

The most straightforward way to analyze temperature perturbations is to simply consider various harmonics of the driving source and consider the corresponding harmonics in the temperature. We can analyze the phase and amplitude of the response to find the effective phase velocity of the perturbation which can in turn be related to parameters in the selected heat flux model. The most common example is to determine χ, the diffusion coefficient that appears in the linearized energy transport equation. The advantages and limitation of this method will be discussed in detail in Section 3.

A more involved approach involves using the perturbed temperature data to compute modulated heat flux at any given point in the perturbation cycle, rather than using the temperature data directly. As before the heat flux can then be related to measured profile parameters and theoretical predictions. The advantages and limitations of this approach will be discussed in more detail.

Both of the mentioned analysis methods are used to probe electron energy transport in a quiescent H mode (QH mode) shot conducted at DIII-D. The nature of the internal transport barrier that is present in the shot is

considered in light of the results.

Table of Contents

List of Tables

List of Figures

Chapter 1

Introduction

Controlled, economically feasible nuclear fusion has been the holy grail of plasma physics for the past 60 years. Understating transport has been and continues to be a key step in bring the promise of fusion to reality. In tokamaks both energy and particle transport exceeds neoclassical predictions; the electron energy channel in particular is larger by about two orders of magnitude. To transition tokamaks successfully from experimental research devices to reliable generators of electric power we have to understand how to maintain the high temperatures and densities prerequisite for thermonuclear fusion.

1.1 Nuclear Fusion

The most practical nuclear reaction compatible with thermonuclear fusion is a deuterium-tritium reaction that produces a 14.1 MeV neutron and a 3.5MeV α particle. This reaction has a larger cross section at accessible temperatures than other candidate reactions. Even this relatively favorable reaction requires tempartures on the order of 10keV. Clearly there will be a large temperature gradient in any reasonably sized thermonuclear fusion

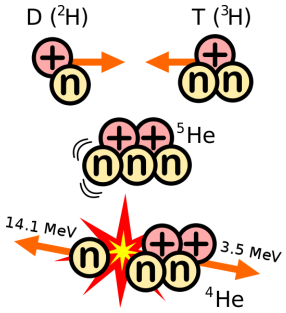

Figure 1.1: D-T reaction

device. Minimizing and understanding heat and particle flow due to this and other sources of free energy present in tokamaks is a major goal of fusion transport studies.

1.2 Tokamaks

Tokamaks provide a set of nested magnetic surfaces that attempt to minimize radial transport and allow plasma to reach high temperature and density required for thermonuclear fusion. To create a magnetic surface requires a magnetic field with a poloidial component, tokamaks achieve this by inducing a toroidal current in the plasma. While existence, stability and evolution of nested magnetic surfaces is nontrivial, in simplest terms when vacuum fields produce the last closed magnetic surface the enclosed magnetic fields generally foliate into 2 dimensional closed nested flux surfaces, rather than islands and regions where a given field line densely fills a three dimensional volume [4].

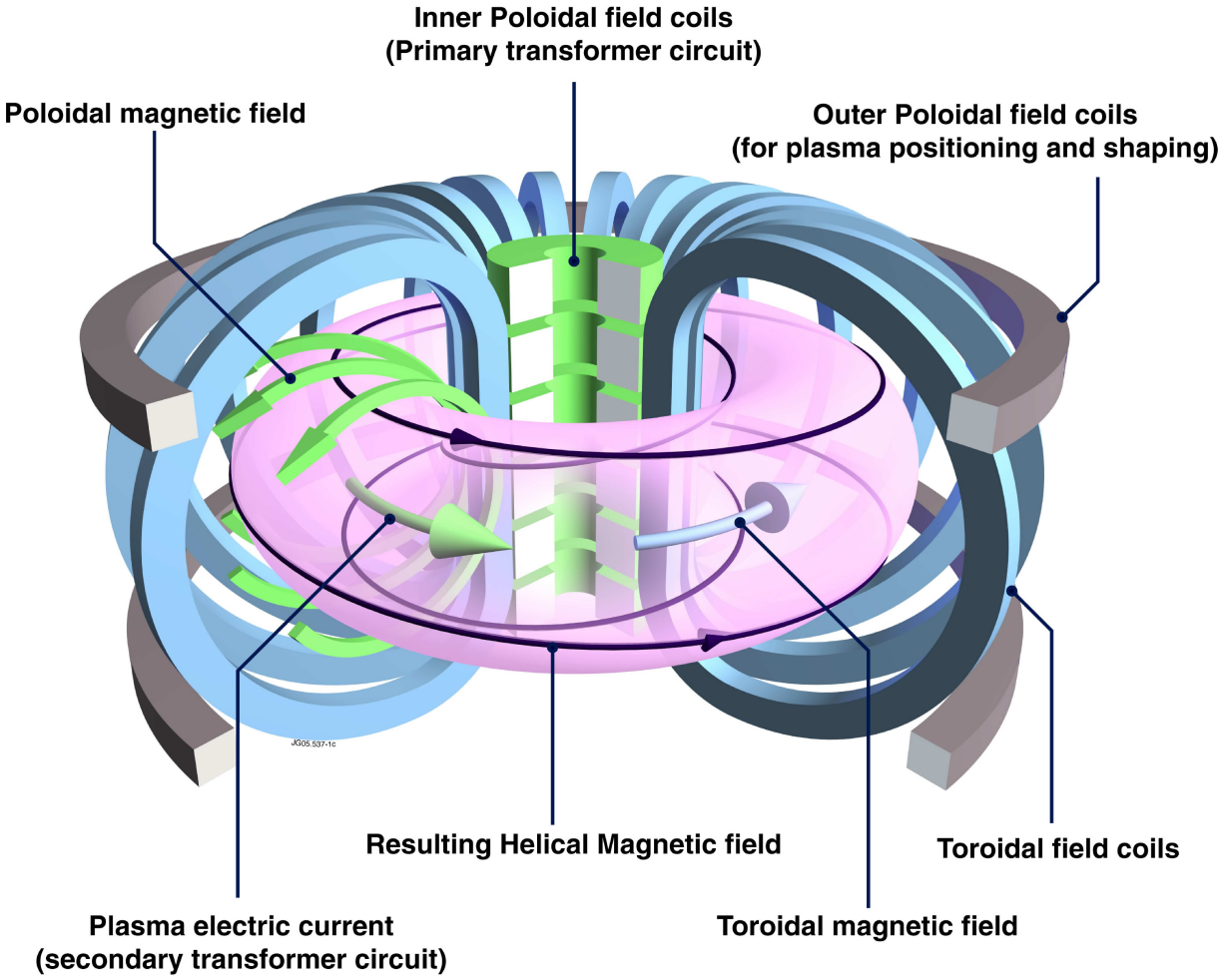

Figure 1.2: Schematic of a tokamak [1]

Chapter 2

Transport

Understanding and controlling radial energy and particle transport in tokamaks is a prerequisite for commercially feasible thermonuclear fusion. There are two main ways to approach this problem. One could start with basic physics principles, and try to build a predictive model that describes how the relevant field and particles evolve in a given situation. In the best case scenario, such a model will presumably be able to describe and predict experimental observations on the basis of fundamental particle and field dynamics. This approach would require a better understanding of turbulent transport than we currently possess. Formulating an experiment that can eliminate candidate theoretical model is nontrivial, since there may be several competing transport mechanism in any given shot.

Alternatively, one can experimentally measure energy and particle flow and see how it changes with experimental plasma parameters, such as power deposition profiles, rotation, temperature gradient and more. Consequently an experimentally useful phenomenology that relates transport to well defined experimental parameters can be synthesized.

The methods are clearly complementary and interdependent. As a simple

example of the relationship between the two approaches we can consider the principle of similarity, which motivated experimental scans in dimensionless parameters [5, 19], and gave a valid parameter space of comparison between different tokamaks. Experiments have encouraged new theoretical developments, such as $E \times B$ shear suppression of turbulence [5], among others. While the fluctuations that drive turbulence maybe be sidestepped in some phenomenological models, at the very least a one dimensional, flux averaged, closed set of fluid equations is necessary to relate observed profiles and events to transport.

2.1 Theoretical Background

While an exact Hamiltonian for every participating particle in tokamak can be written down, for this description be useful we would have to solve $\sim 10^{23}$ nonlinear, coupled differential equations, and make sense of the results. Therefore a statistical description where the state of the system is cast in terms of an ensemble-averaged distribution function $f_\alpha(q, p, t)$, the Vlasov equation, is developed. Vlasov equation (2.1) is an integro-differential nonlinear equation on a six dimensional phase phase, and in most cases it is usually too cumbersome to work with.

$$\partial_t f^\alpha + [H^\alpha, f^\alpha] = C^\alpha(f) \tag{2.1}$$

To simplify the situation, the first three moments (density, momentum and

energy) of the Vlasov equation are considered to create a macroscopic fluid description of the system. Additionally since it is transport along the radial coordinate that is responsible for loss of energy and particles from the reactor we can average over poloidal and toroidal angles to arrive at a set of one dimensional transport equations. While the result is much more tractable than the kinetic description, the evolution of the n^{th} moment is coupled to the $(n+1)$st moment, so various closure methods must be considered.

$$\partial_t n_\alpha = -\frac{1}{r}\partial_r(r\Gamma_\alpha) + S_\alpha \tag{2.2}$$

$$m_\alpha n_\alpha \partial_t V_\alpha = -\frac{1}{r}\partial_r(r\Phi_\alpha) + M_\alpha \tag{2.3}$$

$$\frac{3}{2} n_\alpha \partial_t T_\alpha = -\frac{1}{r}\partial_r[r(Q_\alpha + \frac{5}{2}\Gamma_\alpha T_\alpha)] + P_\alpha \tag{2.4}$$

To close the energy transport equation all the fluxes, $\Gamma_\alpha, \Phi_\alpha$ and Q_α, all well as the moments of the collision operator must be expressed in terms of the first 3 moments of f_α; T_α, n_α and V_α, where α is a particle species label. Determining proper expressions for the various fluxes is one of primary objectives of transport research.

2.1.1 Collisional and Anomalous Transport

Transport can roughly be broken up into two components; collisional and everything else, which is simply called 'anomalous transport'.

Anomalous transport can be driven by changes in the magnetic field topology (ex: island formation, destruction of the nested two dimensional

field structure and formation of a three dimensional space filling stochastic field lines). Additionally anomalous transport can be driven by turbulence, that may not necessarily change the topology of the magnetic field lines.

2.2 Experimental Phenomenology

2.2.1 Local Models

How we describe transport on macroscopic scales is driven by the underlying microscopic reality. The standard approach is to disregard any collective effects and assume the system is in local thermodynamic equilibrium. These assumptions may fail as evidenced by long range fluctuation correlations [5, 7], uphill energy transport [21], and other evidence inconsistent with purely collisional statistics. In any case the simplifying assumptions yield expressions that follow the well know Fourier's Law.

$$\Gamma_\alpha = -D\nabla n + \Gamma_{\alpha,offset} \tag{2.5}$$

$$Q_\alpha = -n_e\chi_e\nabla T_e + Q_{\alpha,offset} \tag{2.6}$$

In general every flux is a function of all gradient of thermodynamics quantities: $\nabla T_e, \nabla n_e, \nabla u, \nabla\Phi$, this can be expressed in compact notation (2.7), where X is vector that contains thermodynamic forces, and J is a vector that contains all fluxes.

$$J_a = L_{ab}\ X_b \tag{2.7}$$

The matrix of transport coefficients relates the microscopic dynamics of the transport processes to the macroscopic picture. We notice that in this description the earlier offset terms can be associated with off-diagonal elements of the transport matrix L_{ab}.

An estimate of transport coefficients based on uncorrelated Coulomb scattering in a toroidal geometry provided a baseline estimate; the best case scenario. Transport predictions based on this mechanism alone are typically 1 to 2 orders of magnitude smaller than experimentally measured values. While assumptions leading to up to equation (2.7) may not always be valid, in the context of this document we proceed to follow that form and parametrize flux by a linear combination of local thermodynamic forces. We hypothesize that the anomalous effects present will be captured by this phenomenology if we carefully measure the transport coefficients, L_{ab} and determine their dependence on profile parameters. The general approach is then to vary the relevant profile parameters, independently of one another if possible, and measure the fluxes in order to determine transport coefficients making up L_{ab}.

If we suspect some portion of heat flux will be driven by local nondiffusive phenomena we can add what are called the "pinch" terms that correspond to convective effects. In equation 2.8 U_e has units of speed and is refered to as heat pinch velocity.

$$Q_\alpha = -n_e \chi_e \nabla T_e - n_e U_e T_e \tag{2.8}$$

Perhaps a fundamentally better macroscopic model can be obtained by

building on a correct statistical description of a turbulent plasma, but this complex subject is beyond the scope of this work.

2.2.2 Nonlocal models

We can consider a generalization of equation (2.5), that allows all regions of the plasma to influence the heat flux at a given location.

$$Q_\alpha = -\chi_{nl}\ \partial_r \int dr' K(r - r') T_e(r') + Q_{\alpha,offset} \tag{2.9}$$

In addition to non-locality in description of fluxes, a non-local generalization of derivatives may be included in formulating a transport model. This approach has seen some success in describing macroscopic transport properties of systems that on the microscopic level are characterized by intermittent flight and trapping events that can be associated with anomalous diffusion[7].

2.3 Transport Barriers

In the context of turbulence driven anomalous transport, transport barriers are believed to facilitate formation of flow shear which in turn decreases the scale length associated with a turbulent eddies. Flow shear can be driven by the radial electric field E_r shear and momentum input from neutral beams. Formation of internal transport barriers depends on the details of the q profile, deposition of heating power, magnetic field strength, current drive,

etc., but there does not appear to be a clear quantitative recipe for producing internal transport barriers that applies to all tokamaks [23]. A given transport barrier may effect different transport channels differently, for example only ion particle transport could be supressed while electron thermal energy and momentum transport are less effected, and transport barriers may be local or broad in radial extent. [2, 10, 15].

Whether a given transport barrier is a sharply localized volume where turbulent eddies are sheared small and transport reduced or is an outer boundary of some larger core region with improved confinement throughout is a question that can be approached experimentally. Experiments conducted in the past at JET and DIII-D have been able to produce localized ITBs in the T_e channel, but have generally found these ITBs to require a more negative shear and increased heating power compared to ion particle and thermal energy channel only ITBs [2, 16] . In addition to discussing some general analysis techniques, one of the aims of this document is to explore an internal transport barrier experiment conducted at DIII-D several years ago, see page 25.

2.4 Measuring Transport

Two methods of estimating transport coefficients are considered. Power balance calculates χ or other parameters found in a chosen closure method by considering the one dimensional energy transport equation (2.4). Once all the profile parameters and power sources that appear in the equation are

found (T_α, n_α, P_α), the fluxes can be determined directly, and transport coefficients calculated. Modulated power balance extends this approach to periodically perturbed plasmas that are otherwise close to equilibrium. This method is discussed in detail in chapter 4.

A simpler approach is to perturb the plasma with a localized modulated power source, find the most powerful harmonics present, and observe how the phase and amplitude at these harmonics evolve as we move away from the point of deposition. Consequentially phase and amplitude profiles can be related to transport by introducing a model that will relate these observations to transport coefficients. In chapter 3 this approach is discussed in greater detail.

While many periods of perturbation are desirable to achieve time dependent profiles with sufficiently smooth derivatives, both techniques are applicable to nonperiodic events.

Chapter 3

Linearized Analysis

The most immediately obvious way to process modulated electron temperature data is to transform the time series data into a Fourier space and consequently find the phase and amplitude of any given harmonic. If the source function is known, then it is straightforward to limit analysis to the harmonics that appear in the source. A model for the heat flux is needed to relate these experimental values to any statements regarding transport. The results of this analysis will depend on the model selected and well as simplifying assumption made along the way. Given phase and amplitude data can be interpreted differently depending on solution method.

One limitation of this method is that the number of unknowns for all but the simplest models will be greater than the number of known quantities. Additional assumptions based on experimental limitations (neglecting higher order derivatives), and driven by the intractable nature of more complicated and realistic models in this context limit the validity of this approach.

3.1 The Basic approach

Consider the case of a 1D fluid approximation of energy transport

$$\frac{3}{2}\partial_t n_e T = -\nabla \cdot Q + P_e \tag{3.1}$$

We can consider a simple form for the heat flux that for now is purely diffusive.

$$Q_e = -n_e \chi_e \nabla T_e \tag{3.2}$$

$$\frac{3}{2} n_e \partial_t T = \nabla \cdot (n_e \chi_e[r] \nabla T_e) \ + P_e \tag{3.3}$$

Given an experiment where field parameters, say just ∇T_e and T_e, are varied around some quasi-stationary state, we can linearize the expression in the perturbed portion of the fields. We will see that even though we can linearize the diffusion-convection with respect to the perturbation, in the end we will have an equation that in general must be solved numerically. Starting with a perturbed energy transport equation.

$$\frac{3}{2} n_e \partial_t (T_e + \delta T_e) = \nabla (n_e \chi_e[r] \nabla (T_e + \delta T_e) \ + (P_e + \delta P_e) \tag{3.4}$$

By linearizing in δ and decomposing the perturbed portion of the equation in a Fourier basis, in time we arrive at a complex nonlinear differential equation that relates perturbed temperature amplitude and phase to χ.

$$\delta T_\omega = \delta T_\omega[r] e^{i(\omega t + \phi[r])}$$

$$\delta P_\omega = \delta P_\omega[r] e^{i(\omega t)}$$

Often the region of deposition is sufficiently narrow that we can simplify the equation significantly if we limit oursevles to regions outside the deposition location, additionally, the imaginary portion of linearized equation 3.4 will not not include the power term anyway. The details of these calculation can be found in many reviews and papers on the subject, see [13, 23].

$$\frac{3\omega}{2} - \frac{\chi[r]\phi'[r]}{r} - \frac{\chi[r]\phi'[r]n'[r]}{n[r]} - \phi'[r]\chi'[r] - \chi[r]\phi''[r] = 0 \qquad (3.5)$$

This nonlinear differential equation is not hard to solve on a computer, all quantities present are experimentally available, albeit the second order derivatives may have large uncertainties and jumps. In reality this approach is rarely implemented; typically a series of further simplifying assumptions are made and the solution is obtained algebraically.

$$\chi[r] = \chi_0$$

$$\delta\phi''_\omega[r] \longrightarrow 0$$

If we assume that χ is constant the situation simplifies. If all these assumptions seem too rough it should be clear that if we desired a closed form analytic solution that directly related local experimental data to χ it's

hard to do better.

$$\chi[r] = \frac{3\ \omega}{4\left(\frac{1}{2r} + \frac{\delta T'_\omega[r]}{\delta T_\omega[r]} - \frac{n'[r]}{2n[r]}\right)\phi'[r]} \tag{3.6}$$

We can better relate this expression to our intuition of transport if we rewrite it in terms of the thermal front velocity and characteristic length scales.

$$V_{th,\omega} = \frac{\omega}{\phi'} \tag{3.7}$$

$$\chi[r] = \frac{3\ V_{th,\omega}}{4\left(\frac{1}{2r} + \frac{1}{L_{\delta T}} - \frac{1}{2L_n}\right)} \tag{3.8}$$

As could be expected, a faster thermal front velocity indicates a larger χ value. As we move radially outward χ tends to increase, and as we approach the point of deposition the thermal velocity will diverge and χ will too; the model breaks down at this location. We can also see that a longer dissipative length $L_{\delta T}$ will translate into a larger χ, describing a more thermally conductive plasma.

The validity of assuming a constant χ to derive $\chi[r]$ is discussed in some detail in [13, 20]. In spite of the apparent contradiction, this approach continues to be a common analysis method when periodic profile parameter perturbations are present.

3.2 Example FFT

To examine how the two approaches to solving the linearized heat transport equation (3.4) differ, we use some well behaved curves to represent

experimental data. In the first two rows of figure (3.1) steady state and perturbed electron temperature profiles, along with the phase difference $\phi[r]$ with respect to the ECH source are plotted. Two possibilities are overlayed, a case with a strong localized ITB around $\rho = .3$, evidenced by rapid damping of the perturbed temperature and slowdown of phase velocity, and a shot lacking any strong localized features expect perhaps at the point of power deposition. The pictured profiles are used to calculate χ both by integrating equation (3.5) and by using the simpler formula (3.6), the results are shown on the bottom row. While this is not a simulation, and there is not a "real" χ to compare the results to, it is sufficient to notice that the two methods, while yielding transport coefficients that are of the same order of the magnitude, are sufficiently different to consider using both in post-experimental analysis.

As pointed out earlier and seen in figure (3.1) the simple solution of χ_e diverges rapidly near the power deposition location, while the more complete solution does not. While the non-local solution does detect the ITB in this case, it also tends to diverge immediately inside the ITB, this feature is more pronounced for more spatially localized profile features.

3.3 Advantages and limitations

This method is simple and its product is unambiguous; phase and amplitude of a given harmonic as a function of displacement that are in turn used to compute thermal diffusivity. Compared to modulated power, balance the

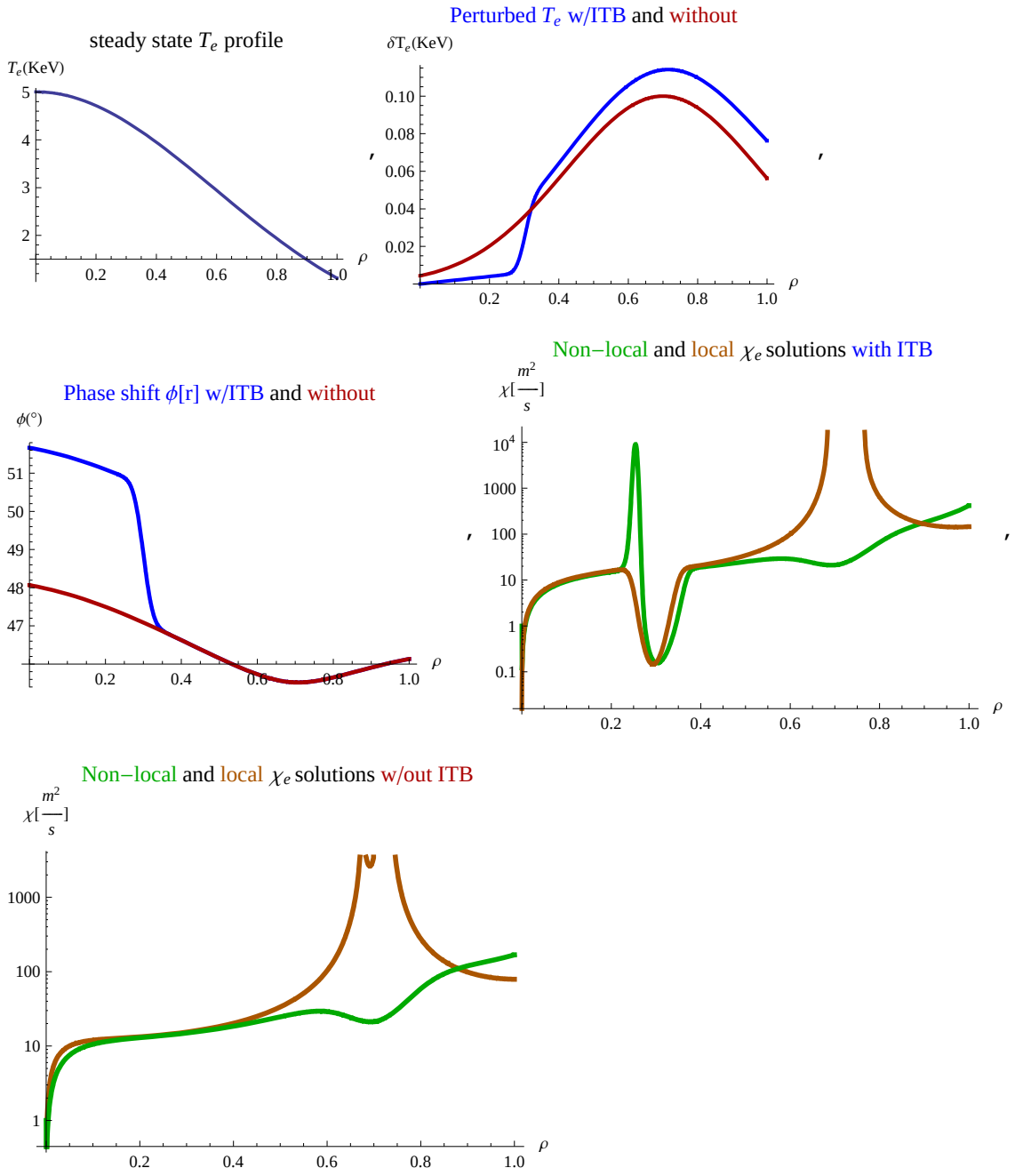

Figure 3.1: Solving equation (3.5) numerically may be worth the effort.

simpler version of this method as expressed in equation (3.6) is better able to determine local changes in diffusivity, making itself especially useful in the context of internal transport barrier experiments [15, 16], however the method is inherently inconsistent for large $\partial_r \chi$. A more complete approach as expressed in equation (3.5) is inherently non-local, so while technically it is a more accurate description of thermal diffusivity, it may be limited by experimental noise and may be limited in its ability to detect spatially localized transport changes. Additional tests of this method are needed to assess it's value and validity. Initial application to experimental data seems to yield reasonable results.

One major simplification of this approach is the linearization of the energy transport equation around some steady state equilibrium; it has been shown experimentally that this approach may be inadaqute, even when the pertubed magnitudes are separated from steady state by an order of magnitude [9]. We should point out that in all but the most limiting case of $q_{offset} = 0$ and $\frac{d\chi_e}{d\nabla T_e} = 0$, the best we can hope for with this approach is to find χ_e^{pert} at a particular point in the macroscopic state space of the plasma. One may call the transport coefficient computed in such manner transient [5]. Additionally any method where the results depend on the model one chooses introduce bias; ideally the experiment can rule out a model rather than simply find a coefficient that makes the observed data fit the desired model.

Chapter 4

Modulated power balance

Modulated power balance is a time dependent generalization of the power balance method. This approach computes the heat flux, Q_α, without introducing any models. Additionally the method allows to independently measure ECH power deposition, the result may be compared to ray tracing codes, such as TORAY [9]. Unlike the analysis discussed in chapter 3 this approach does not assume linearity.

4.1 The Basic Approach

Consider traditional power balance analysis. Starting with the energy transport equation.

$$\frac{3}{2}n_a\frac{\partial T_e}{\partial t} = -\frac{1}{r}\frac{\partial}{\partial r}[r(Q_a + \frac{5}{2}\Gamma_e T_e)] + P_e \tag{4.1}$$

rearrange and integrate radially outward

$$\iint d\psi\ dS[\psi]\nabla_\psi \cdot (Q_e[\psi] + \frac{5}{2}\Gamma_e T_e[\psi]) = \int dV[\psi](P_e - \frac{3}{2}n_a\frac{\partial T_e}{\partial t})$$

$$Q_e[\psi] + \frac{5}{2}\Gamma_e T_e[\psi] = \frac{\int_0^{\psi'}\int d\psi\ dS[\psi'](P_e - \frac{3}{2}n_a\frac{\partial T_e}{\partial t})}{S[\psi]} \tag{4.2}$$

where $d\psi\ dS[\psi]$ is the element of volume defined by the surface area function $S[\psi]$ and the radial displacement by the differential $d\psi$ of the magnetic flux. In a simplified situation where $S[\psi] = 2\pi\psi L$ and the electrons are not moving across flux surfaces the above simplifies

$$Q_e[\rho] = \frac{\int_0^\rho d\rho' \rho' (P_e[\rho'] - \frac{3}{2} n_a[\rho'] \frac{\partial T_e[\rho']}{\partial t})}{\rho} \tag{4.3}$$

In a steady state situation time derivative will vanish and assuming we know all the sources and sinks that comprise $P_e[\rho]$ as well the magnetic geometry it is straightforward to compute $Q_e[\rho]$. Typically we are interested in how Q_e evolves in time in response to changing thermodynamic forces. In practice it may be difficult to compute the time derivative term in equation (4.3) accurately, hence it is desirable to calculate some averaged plasma response to a periodic perturbation, if the perturbation is not periodic but is nevertheless repeated coherent integration may an alternative technique for averaging the plasma response.

4.2 Inducing a model and measuring transport coefficients

Theoretically Q_e could be a function of any number of variables but if we postulate that its evolution over the modulation cycle is driven by n independent thermodynamic forces we can identify the task of determining the transport coefficients with projecting Q_e's time history onto an n dimensional manifold where Q_e must be expressible as a one-to-one function

of the relevant thermodynamic forces. First several variables that are believed to provide a good basis for Q_e's evolution in time are supplied. Electron cyclotron heating by it's design most strongly and directly effects the (surprise) electron temperature profile; we can limit ourselves to functions of ∇T_e and T_e as potential independent variables.While ∇T_e and T_e may not be entirely orthogonal function, at every flux surface where their inner product is non-vanishing they do span a 2-dimensional space, which is typically sufficient to define Q_e as one-to-one function of (∇T_e and T_e). If the simple heat flux model of $Q_e = -\chi \nabla T_e$ with $\frac{\partial \chi}{\partial \nabla T_e} = 0$ is to be believed we only need one variable, ∇T_e to parametrize Q_e evolution over a cycle of modulation and χ is found by the method of least squares.

One parameter of particular practical interest is the electron temperature threshold, ∇T_e^c. When ∇T_e exceeds this threshold transport through the electron channel becomes turbulent and grows quickly with increasing ∇T_e. While the physics of the transition to turbulence is interesting, any future fusion based electrical energy generator would be careful to avoid exceeding this critical threshold and needlessly losing energy and lowering core temperature. The Horton model, expressed in equation (4.4), based on ETG drift wave turbulence predicts an explicit value for the critical gradient. Power balance analysis of experiments at the Tore Supra tokamak have found good agreement between this model's predictions and experimental

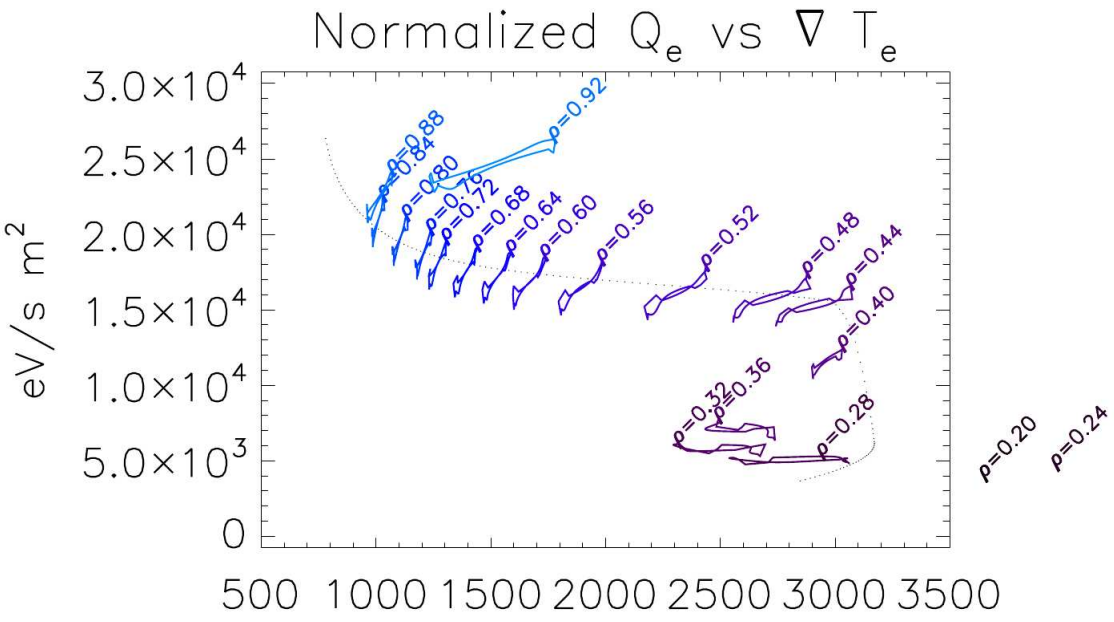

Figure 4.1: Q_e vs ∇T_e curves for an L-mode shot(105677) with modulated ECH

results [11, 22].

$$\chi_e = C_e^{em} \frac{c^2}{\omega_{pe}^2} \frac{v_e}{(L_{T_e} R)^{\frac{1}{2}}} \tag{4.4}$$

$$\nabla T_e^2 = 1.88 \frac{sT_e}{qR} (1 + Z_{eff} \frac{T_e}{T_i}) \tag{4.5}$$

$$Q_e = -n_e \chi_e (\nabla T_e - \nabla T_e^c) \tag{4.6}$$

Principal component analysis (PCA) is the formal mathematical procedure of finding the most efficient linear basis in which to represent a given data set. PCA will not be reviewed in any detail here, many excellent guides are available [14]. Suffice to say that PCA provides an economical way to

compute diffusive and non-diffusive transport coefficients. In short given a model of form $Q_e = -n_e\chi_e\nabla T_e + n_e U_e T_e$, χ_e and D_e can be found.

4.3 Measuring power deposition

Given the reasonable restriction of expressing modulated Q_e as a one-to-one function of ∇T_e and T_e we have to deal with the experimental possibility that our data will fail to satisfy this constraint. As an example, when the power deposition is a simple on-off modulation one problem experienced is a sharp discontinuity in the measured Q_e at the on/off time. Since neither ∇T_e or T_e will change quickly enough at this point in time to be useful as independent variables to parametrize Q_e in the sense of section (4.2) we have reconsider how we calculate Q_e in the first place. To amend this problem we change the spatial profile of the power deposition in equation (4.3) as needed in order to come as close as possible to a continuous description of Q_e in time, as prerequisite to parametrizing Q_e by ∇T_e and T_e. The resulting P_e can then be considered an independent means of verifying power deposition. Figure 4.2 shows the integral term in equation (4.3) before (dashed blue line) and after power deposition has be altered to enforce a continuous heat flux in time.

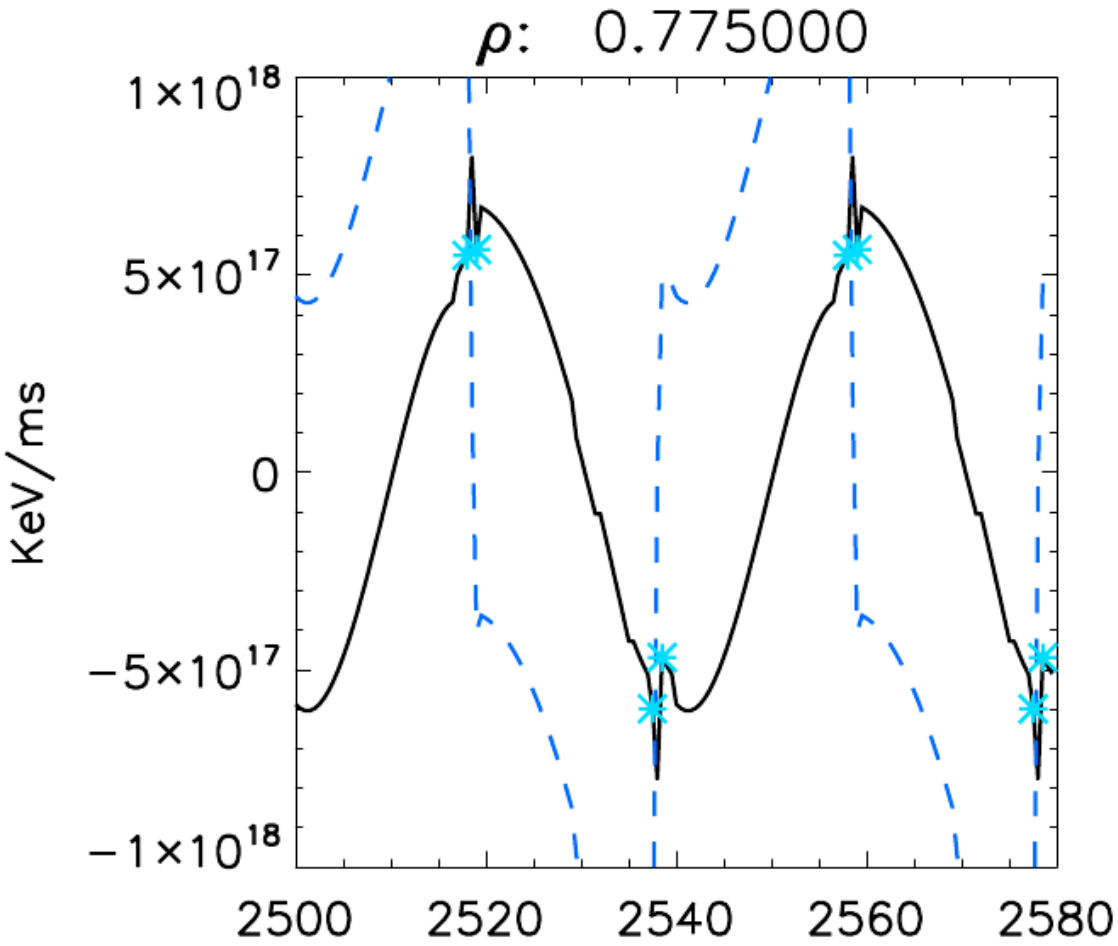

Figure 4.2: Enforcing a continuous heat flux, solid line is corrected integrated power

Chapter 5

Example: QH Mode with Modulated ECH

5.1 Experiment description

Quiescent H-mode shots (QH-mode) are ITB shots characterized by an edge harmonic oscillation and an internal transport barrier. Edge harmonic oscillation (EHO) is believed to play a role in suppressing ELMS by enhancing particle transport near the edge and thereby reducing the edge pressure gradient [15, 23]. In the presence of EHO, edge pressure profiles become stiff; as the plasma gets more hot near the core the mechanism responsible for regulating particle exhaust near the edge is able to keep up and maintain the pressure gradient below some critical threshold. Edge particle transport is increased while energy transport is similar to that of more conventional H-mode shots. Whatever the edge particle mechanism happens to be, it cannot be simply identified directly as EHO. For a detailed analysis of QH-mode experiment please see [15].

Some information regarding the two shots considered; shot 119341 and shot 105677, is summarized in Table 5.1. Shot 105677 is an L-mode shot designed to measure profile stiffness. These two experiments, with very different transport properties provide a convenient context in which to examine

analysis techniques presented in this document.

shot	119341	105677
modulated ech power	.8 (MW)	1 (MW)
deposition radius	.7	.4
ECH modulation f_0	25 (Hz)	25 (Hz)
neutral beam heating	9.03 (MW)	8.95(MW)
max n_e	5.4×10^{19} $(\frac{1}{m^3})$	4×10^{19} $(\frac{1}{m^3})$
current	1.30 (MA)	.83 (MA)
B_T	2 (T)	2 (T)

Table 5.1: shot information

5.2 Results

5.2.1 Power Deposition

As described in chapter 4., we can calculate power deposition in a shot with modulated ECH by demanding a that the heat flux at a given radial location is a smooth function, free of sharp jumps. The spread in the power deposition could be attributed to the edge harmonic oscillation found in shot 119341. EHO has a frequency on the order of tens of kHz, whereas ECH heating is modulated at frequency of 25 Hz, The large discrepancy in the two frequencies would allow the EHO to modulate the density and the refraction angle of the ECH beam thousands of times time during one period of ECH modulation.

As seen in Figure 5.1, the deposition is significantly broadened. A control shot 105677 is considered in figure 5.2. While some significant broadening is observed, the deposition profile is still significantly more focused than the

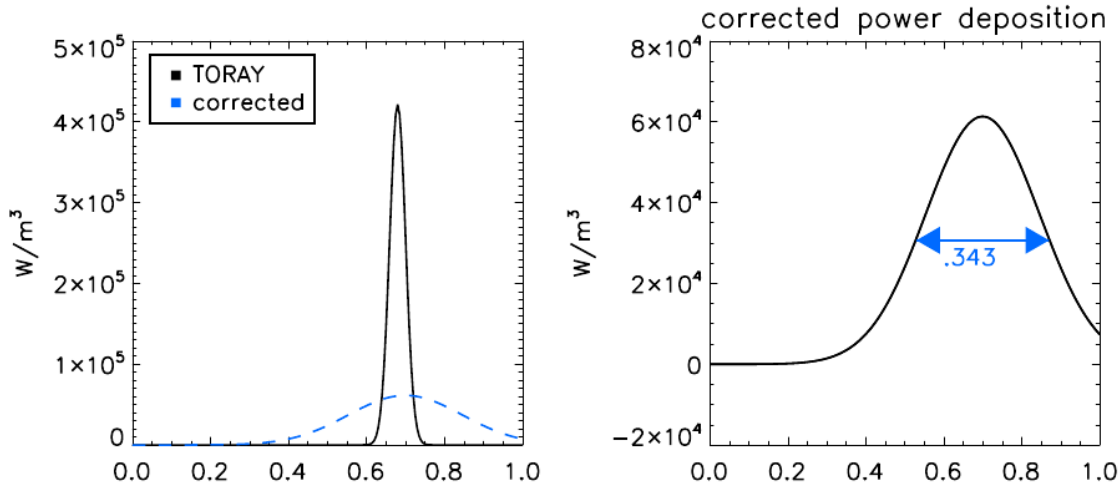

Figure 5.1: Corrected deposition shows a broader profile, possibly due to EHO refracting the beam for discharge 119341

QH-mode profile .

If a mode of operation analogous to the QH-mode is to be successfully adapted to ITER, the potential of RF power broadening due to the presence of EHO or nonlinearities in the plasma response to external heating will have to be taken into consideration. For example, the use of modulated ECH to stabilize neoclassical tearing modes, a technique that depends on accurate power deposition, may be effected. A detailed study of potential issues associated with broadened power deposition would be useful.

5.2.2 Transport Features

The QH-mode shot considered appears to lack a localized internal transport barrier in the electron channel. However a general reduction of electron

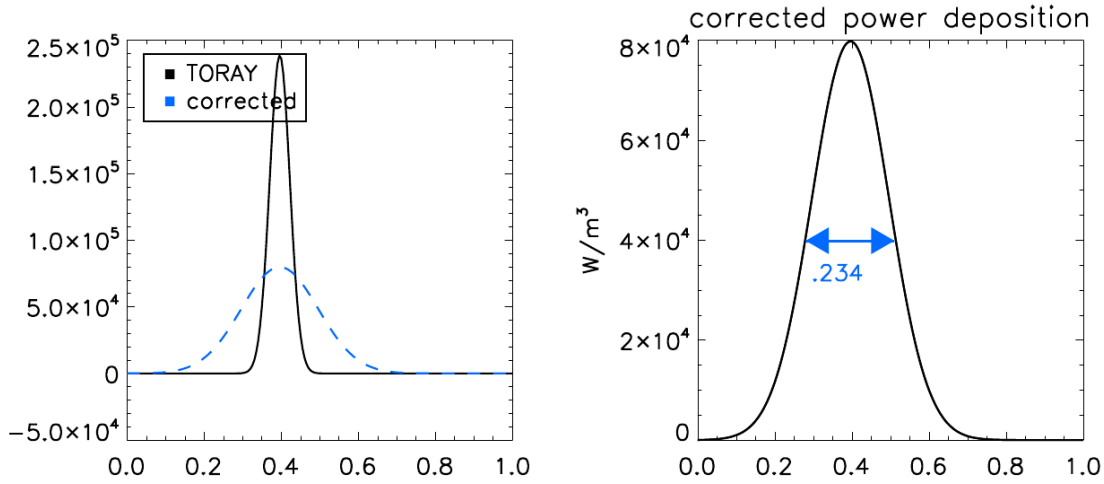

Figure 5.2: Significant broadening is observed in an EHO-free, L-mode shot in discharge 105677

energy transport is observed, especially near the core where ion transport levels approach neoclassical values.

All methods of computing the thermal transport coefficient considered yielded similar results. It is notable that the integrated linearized analysis consistently produced a $\chi[r]$ that grew more slowly in the radially outward direction than other approaches; perhaps we need to examine the effects of noise in phase and amplitude data on this method.

5.3 Future Work

At the present moment the algorithm that searches, through possible applied power profiles, as described in section 4.3, will at times be overly sensitive to

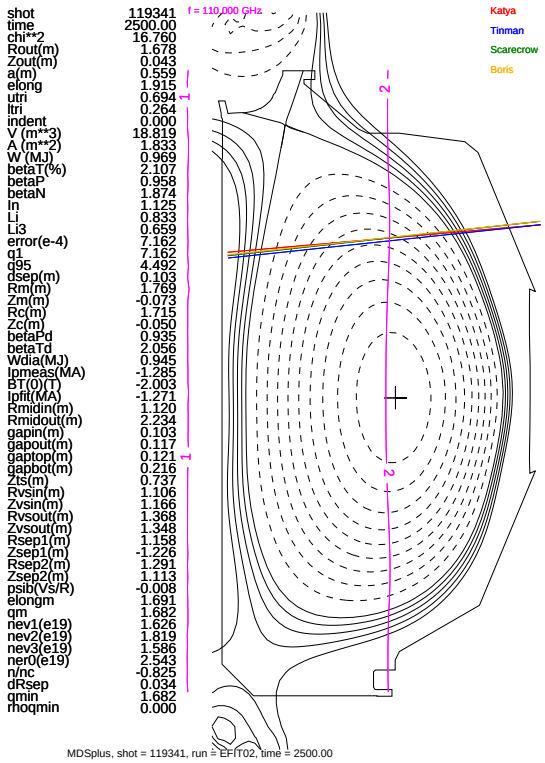

Figure 5.3: The ECH beam may be refracted as it passes through the edge region

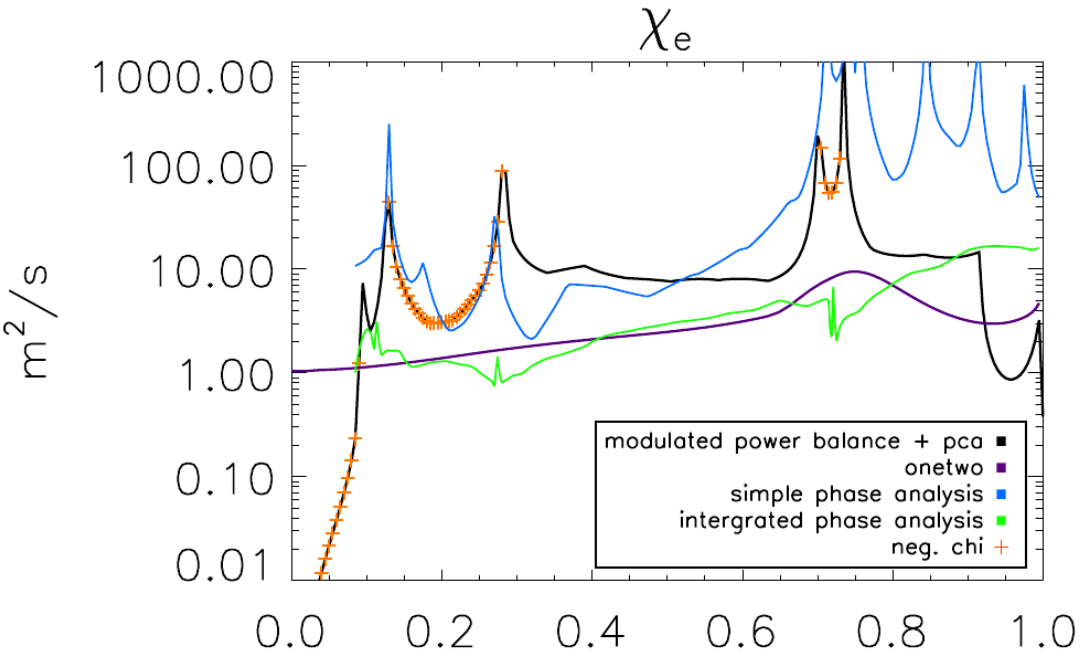

Figure 5.4: QH-mode shot 119341 shows significant reduction of electron energy transport, steady-state power balance analysis peformered in ONETWO yields $\chi_e < 10\left(\frac{m^2}{s}\right)$ everywhere in the plasma

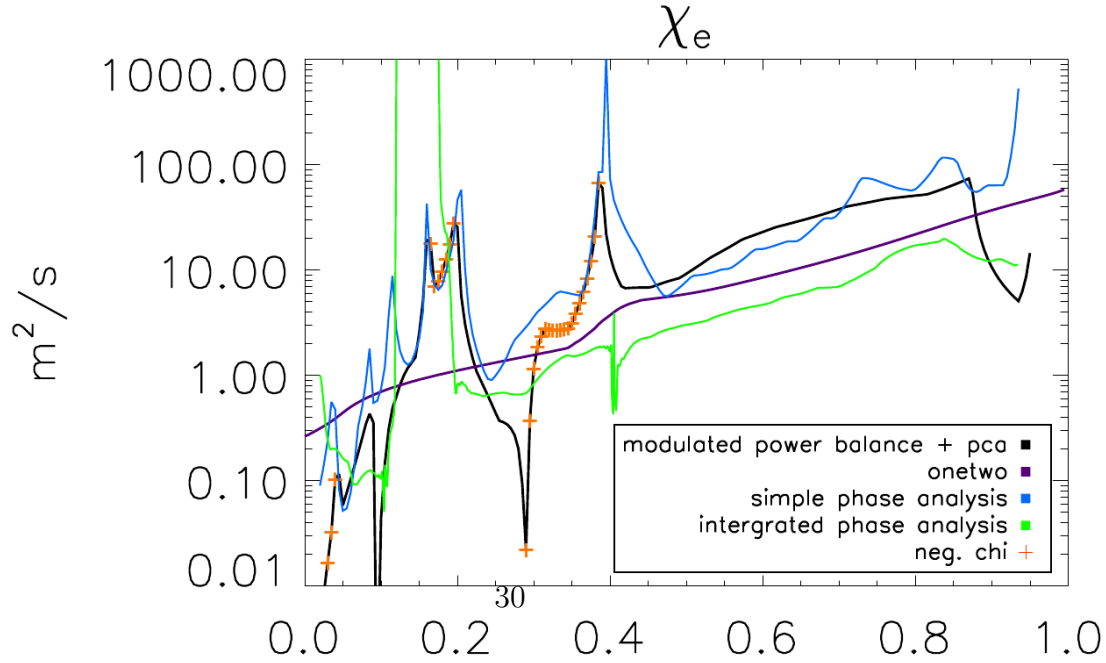

Figure 5.5: L-mode shot 105677 shows larger thermal transport coefficients than the QH-mode

the initial starting point in this search. For reliable application this issue must be resolved.

In future ITB experiments it may be advantageous to apply modulated ECH close to the core region, in order to maximize the extent of a region where the simplest models of ECH power application are valid. An ITB experiment that couples modulated ECH with a scan in steady state quantities that determine the character of the transport barrier would shed some light on the physics as well as experimental control of ITBs. The methods reviewed in this document are quite general and can be easily extended to include electron-ion thermal coupling. Momentum transport may also be added but requires introducing poorly measured flow velocities of the hydrogenic plasma.

Bibliography

[1] 4_diagrama del principio tokamak (imagen jet).jpg. [Online; accessed 10-July-2006].

[2] Observation of simultaneous internal transport barriers in all four transport channels and correlation with turbulence behaviour in ncs discharges on diii-d.

[3] F.Ryter A. Manini, J.-M. Moret and the ASDEX Upgrade Team. Signal processing techniques based on singular value decomposition applied to modulated ech experiments. *Nuclear Fusion*, 43(490-511), 2003.

[4] Allen H. Boozer. Physics of magnetically confined plasmas. *Reviews of Modern Physics*, 76, October 2004.

[5] Benjamin A. Carreras. Progress in anomalous transport research in toroidal magnetic confinement devices. *IEEE Transactions on Plasma Science*, 25(6), December 1997.

[6] V. Naulin J.J. Rasmussen D. del Castillo-Negrete, P. Mantica and JET EFDA contributors. Fractional diffusion models of non-local perturbative transport: numerical results and application to jet experiments. *Nuclear Fusion*, 48, 2008.

[7] D. del Castillo-Negrete, B. Carreras, and V. Lynch. Nondiffusive transport in plasma turbulence: A fractional diffusion approach. *Physical Review Letters*, 94, 2005.

[8] M Beurskens S Cirant G T Hoang G M D Hogeweij F Imbeaux A Jacchia P Mantica W Suttrop F Ryter, C Angioni and G Tardini. Experimental studies of electron transport. *Plasma Physics and Controlled Fusion*, 43(A323-A338), 2001.

[9] K. W. Gentle, T. C. Luce M. E. Austin, J. C. DeBoo, and C. C. Petty. Electron energy transport inferences from modulated electron cyclotron heating in diii-d. *Physics of Plasmas*, 13(012311), 2006.

[10] P. Gohil. Dynamics of the formation, sustainment and destruction of transport barriers in magnetically contained fusion plasmas. *Plasma Physics and Controlled Fusion*, 44, 2002.

[11] Bourdelle C. Garbet X. Ottaviani M. Horton W., Hoang G.T. and Colas L. Electron transport and the critical temperature gradient. *Physics of Plasmas*, 11.

[12] B. A. Carreras I. Calvo, R. Snchez and B. Ph. van Milligen. Fractional generalization of ficks law: derivation through continuous-time random walks, 2008.

[13] A. Jacchia, F. De Luca P. Mantica, and G. Gorini. Determination of diffusive and nondiffusive transport in modulation experiments in plasmas.

Physics of Fluids B, 11, November 1991.

[14] I Jolliffe. *Principal Component Analysis*. Springer -Verlag New York Inc., 2nd edition, 2002.

[15] b W. P. West 1 E. J. Doyle 2 M. E. Austin 3 T. A. Casper 4 P. Gohil 1 C. M. Greenfield 1 R. J. Groebner 1 A. W. Hyatt 1 R. J. Jayakumar 4 D. H. Kaplan 1 L. L. Lao 1 A. W. Leonard 1 M. A. Makowski 4 G. R. McKee 5 T. H. Osborne 1 P. B. Snyder 1 W. M. Solomon 6 D. M. Thomas 1 T. L. Rhodes 2 E. J. Strait 1 M. R. Wade 7 G. Wang 2 K. H. Burrell, 1 and L. Zeng2. Advances in understanding quiescent h-mode plasmas in diii-d. *Physics of Plasmas*, 12, 2005.

[16] P. Mantica, D. VanEester, X. Garbet, F. Imbeaux, L. Laborde, M. Mantsinen, A. Marinoni, D. Mazon, D. Moreau, N. Hawkes, E. Joffrin, V. Kiptily, S. Pinches, A. Salmi, S. Sharapov, A. Thyagaraja, I. Voitsekhovitch, P. deVries, and K.-D. Zastrow. Probing internal transport barriers with heat pulses in jet. *Physical Review Letters*, 96:095002, 2006.

[17] Panoptik. D-t fusion.svg, 2007. [Online; accessed 10-July-2006].

[18] Michiel Peters. *Electron Heat Transport in Current Carrying and Currentless Thermonuclear Plasmas*. PhD thesis, January 1996.

[19] C.C. Petty. Sizing up plasmas using dimensionless parameters. *Physics of Plasmas*, 15, 2008.

[20] X. L. Zou S. P. Eury, E. Harauchamps and G. Giruzzic. Exact solutions of the diffusion-convection equation in cylindrical geometry. *PHYSICS OF PLASMAS*, 12(102511), 2005.

[21] J. C. de Bass T. C. Luce, C. C. Petty. Inward energy transport in tokamak plasmas. *Physical Review Letters*, 68(1), January 1992.

[22] P.J. Morrison A. Wurm J.H. Kim J.C. Perez J. Pratt G.T. Hoang B.P. LeBlanc W. Horton, H.V. Wong and R. Ball. Temperature gradient driven electrontransport in nstx and tore supra. *Nuclear Fusion*, 45, 2005.

[23] John Wesson. *Tokamaks*. Oxford University Press, 2004.

Vita

Dmitry Meyerson was born in Moscow, Russia on 15 April 1983, the son of Dr. Felix Meerson and Elena Vorontsova. He received the Bachelor of Arts degree in Physics from Cornell University in December of 2005. He applied to the University of Texas at Austin for enrollment in their physics program. He was accepted and started graduate studies in August, 2006.

Permanent address: dmitry.meyerson@gmail.com

This thesis was typeset with LaTeX[†] by the author.

[†]LaTeX is a document preparation system developed by Leslie Lamport as a special version of Donald Knuth's TeX Program.